0026-895X/08/7304-1072–1084$20.00
MOLECULAR PHARMACOLOGY
Copyright © 2008 The American Society for Pharmacology and Experimental Therapeutics
Mol Pharmacol 73:1072–1084, 2008

Vol. 73, No. 4
43844/3318247
Printed in U.S.A.

Madin-Darby Canine Kidney II Cells: A Pharmacologically Validated System for NPC1L1-Mediated Cholesterol Uptake

Adam B. Weinglass, Martin G. Köhler, Emmanuel O. Nketiah, Jessica Liu, William Schmalhofer, Anu Thomas, Brande Williams, Lindsey Beers, Lauren Smith, Mike Hafey, Kelly Bleasby, Joseph Leone, Yui Sing Tang, Matthew Braun, Feroze Ujjainwalla, Margaret E. McCann, Gregory J. Kaczorowski, and Maria L. Garcia

Departments of Ion Channels (A.B.W., M.G.K., E.O.N., J.L., W.S., A.T., B.W., L.B., L.S., G.J.K., M.L.G.), Drug Metabolism (M.H., K.B., Y.S.T., M.B.), Medicinal Chemistry (J.L., F.U.), and Pharmacology (M.E.M.), Merck Research Laboratories, Rahway, New Jersey

Received November 26, 2007; accepted January 9, 2008

ABSTRACT

Absorption of dietary cholesterol in the proximal region of the intestine is mediated by Niemann-Pick C1-like protein (NPC1L1) and is sensitive to the cholesterol absorption inhibitor ezetimibe (EZE). Although a correlation exists between EZE binding to NPC1L1 in vitro and efficacy in vivo, the precise nature of interaction(s) between NPC1L1, EZE, and cholesterol remain unclear. Here, we analyze the direct relationship between EZE analog binding to NPC1L1 and its influence on cholesterol influx in a novel in vitro system. Using the EZE analog [^{3}H]AS, an assay that quantitatively measures the expression of NPC1L1 on the cell surface has been developed. It is noteworthy that whereas two cell lines (CaCo-2 and HepG2) commonly used for studying NPC1L1-dependent processes express almost undetectable levels of NPC1L1 at the cell surface, polarized Madin-Darby canine kidney (MDCKII) cells endogenously express 4×10^5 [^{3}H]AS sites/cell under basal conditions. Depleting endogenous cholesterol with the HMG CoA reductase inhibitor lovastatin leads to a 2-fold increase in the surface expression of NPC1L1, supporting the contention that MDCKII cells respond to changes in cholesterol homeostasis by up-regulating a pathway for cholesterol influx. However, a significant increase in surface expression levels of NPC1L1 is necessary to characterize a pharmacologically sensitive, EZE-dependent pathway of cholesterol uptake in these cells. Remarkably, the affinity of EZE analogs for binding to NPC1L1 is almost identical to the IC_{50} blocking cholesterol flux through NPC1L1 in MDCKII cells. From a mechanistic standpoint, these observations support the contention that EZE analogs and cholesterol share the same/overlapping binding site(s) or are tightly coupled through allosteric interactions.

Whole-body cholesterol homeostasis is maintained through three major pathways: de novo synthesis, intestinal absorption, and biliary excretion. Absorption of dietary and biliary cholesterol occurs in the proximal jejunum of the small intestine (Grundy, 1983), and this process is blocked by ezetimibe, a drug used for the treatment of hypercholesterolemia. Ezetimibe, a potent cholesterol and phytosterol uptake inhibitor, effectively lowers circulating plasma cholesterol in humans by 15 to 20% (Bays et al., 2001; Dujovne et al., 2002; Knopp et al., 2003) and its coadministration with HMG CoA reductase inhibitors (statins), inhibitors of cholesterol synthesis, leads to further reductions in cholesterol plasma levels (Davidson et al., 2002; Gagné et al., 2002; Ballantyne et al., 2003; Kerzner et al., 2003; Melani et al., 2003).

By searching expressed sequence tag databases for the presence of a sterol-sensing domain, a plasma membrane secretion signal, and enriched expression in intestinal enterocytes, the Niemann-Pick C1-Like 1 (NPC1L1) protein was identified in 2004 as a potential candidate gene product for the ezetimibe-sensitive pathway of cholesterol absorption. Mice deficient in NPC1L1 were found to have ~70% reduction in sterol absorption, the residual component being in-

Article, publication date, and citation information can be found at http://molpharm.aspetjournals.org.
doi:10.1124/mol.107.043844.

ABBREVIATIONS: NPC1L1, Niemann-Pick C1-Like 1; MDCKII, Madin-Darby canine kidney II; HEK, human embryonic kidney; DMEM, Dulbecco's modified Eagle's medium; FBS, fetal bovine serum; EZE, ezetimibe; EZE-gluc, ezetimibe glucuronide; ent-1, EZE-gluc-enantiomer; PS, 4-[(2*S*,3*R*)-3-[(3*S*)-3-(4-fluorophenyl)-3-hydroxypropyl]-1-(4-{3-[(methylsulfonyl)amino]prop-1-yn-1-yl}phenyl)-4-oxoazetidin-2-yl]phenyl-β-D-glucopyranosiduronic acid; AS, 4-[(2*S*,3*R*)-3-[(3*S*)-3-(4-fluorophenyl)-3-hydroxypropyl]-1-(4-{3-[(methylsulfonyl)amino]propyl}phenyl)-4-oxoazetidin-2-yl]phenyl β-D-glucopyranosiduronic acid; HPLC, high-performance liquid chromatography; PCR, polymerase chain reaction; QRT-PCR, quantitative real-time PCR; PBS, phosphate-buffered saline; βmCD, methyl-β-cyclodextrin; LPDS, lipoprotein-deficient serum; Ch, cholesterol.

sensitive to ezetimibe (Altmann et al., 2004). These findings convincingly demonstrated that NPC1L1 is a critical component of cholesterol uptake in enterocytes (Altmann et al., 2004). With the use of enterocyte brush-border membranes from several species, including NPC1L1 knockout mice, or membranes derived from cells expressing recombinant NPC1L1, radioligand binding studies with ezetimibe convincingly established NPC1L1 as the direct target of ezetimibe in vivo (Garcia-Calvo et al., 2005).

Probing the molecular mechanism of NPC1L1 action is complicated by the difficulties associated with culturing enterocytes in vitro (Simon-Assmann et al., 2007). Therefore, researchers have developed a variety of alternative systems, including brush-border membrane vesicles from enterocytes (Knöpfel et al., 2007; Labonté et al., 2007), cell lines heterologously expressing recombinant NPC1L1 (Davies et al., 2005; Iyer et al., 2005; Yu et al., 2006; Brown et al., 2007; Hawes et al., 2007), cell lines endogenously expressing NPC1L1, such as CaCo-2 (Davies et al., 2005; During et al., 2005; Garmy et al., 2005; van der Veen et al., 2005; Duval et al., 2006; Sané et al., 2006; Alrefai et al., 2007; Field et al., 2007; Mathur et al., 2007; Yamanashi et al., 2007) and HepG2 (Davies et al., 2005; Yu et al., 2006), and functional complementation in *Caenorhabditis elegans* (Smith and Levitan, 2007). By overexpressing NPC1L1 in McArdles RH7777 hepatoma cells (Yu et al., 2006) and CaCo-2 enterocyte-like cells (Yamanashi et al., 2007), it has been possible to establish assays with which to monitor a component of EZE-sensitive cholesterol influx (Yu et al., 2006; Yamanashi et al., 2007). However, pharmacological validation of these cell lines and insight into the mechanism by which EZE analogs inhibit cholesterol flux through NPC1L1 remain quite limited.

In this study, we attempt to address the relationship between binding of EZE analogs to NPC1L1 and their effect on cholesterol flux in vitro, using a combination of novel tools. A cell-based binding assay that can accurately determine the surface expression of NPC1L1 has been established with the use of the high-affinity EZE analog, [^{3}H]AS. It is noteworthy that whereas CaCo-2 and HepG2 cells display no discernible [^{3}H]AS binding, a polarized dog kidney cell line (MDCKII) was found to express significant amounts of endogenous NPC1L1 at the cell surface in a manner that can be modulated in response to changes in endogenous cholesterol levels. Overexpression of either dog or human NPC1L1 in MDCKII cells provides an assay with which to monitor cholesterol flux, which is pharmacologically modulated by EZE analogs. It is noteworthy that the affinity of EZE analogs for binding to NPC1L1 is almost identical to their IC_{50} values, blocking cholesterol flux through NPC1L1. Viewed from a mechanistic perspective, these data support the notion that EZE analogs and cholesterol share the same/overlapping binding site(s) on NPC1L1 or that these sites are tightly coupled through allosteric interactions.

Materials and Methods

Materials. Restriction enzymes and Pfusion polymerase were from New England Biolabs (Ipswich, MA). pCDNA5-FRT-TOPO, pCDNA5-FRT, SuperScript II, and STBL2 competent cells were purchased from Invitrogen (Carlsbad, CA,). Synthetic oligonucleotides were synthesized by Integrated DNA Technologies, Inc. (Coralville, IA). Tri Reagent for RNA preparation was from Molecular Research Center (Cincinnati, OH). dNTPs were purchased from Roche Diagnostics (Indianapolis, IN), RNeasy columns from QIAGEN (Valencia, CA), and Chromaspin columns from Clontech (Mountain View, CA). Dye terminator sequence reactions were performed with the ABI Big Dye 3.1 sequencing kit and analyzed with an ABI3100 genetic analyzer, both from Applied Biosystems (Foster City, CA). Human embryonic kidney (HEK) 293, HepG2, LLC-PKI, and CaCo-2 cell lines were from American Type Culture Collection (Manassas, VA). MDCKII cells were from Dr. Piet Borst (Netherlands Cancer Institute, Amsterdam, The Netherlands) (Louvard, 1980) and TsA201 cells were a gift of Dr. Robert DuBridge (Pdl Biopharm Inc., Freeman, CA). Fugene6 transfection reagent was from Roche. Generation and maintenance of a stable cell line expressing rat NPC1L1 in HEK293 cells (rNPC1L1/HEK293) (Garcia-Calvo et al., 2005), and procedures for handling TsA201 cells and their transfection with FuGENE6 have been described previously (Hanner et al., 2001). LLC-PKI cells were maintained in medium 199 + GlutaMax, CaCo-2 and MDCKII cells were maintained in in DMEM + Glutamax (Sigma, St. Louis, MO), and HepG2 cells were maintained in Eagle's minimum essential medium. All media were supplemented with 10% FBS, penicillin, and streptomycin, and cells were grown at 37°C in 5% CO_2.

Ezetimibe (EZE), ezetimibe glucuronide (EZE-gluc), and the EZE-gluc-enantiomer (ent-1) were prepared as described previously (Garcia-Calvo et al., 2005). The propargyl sulfonamide, 4-[(2*S*, 3*R*)-3-[(3*S*)-3-(4-fluorophenyl)-3-hydroxypropyl]-1-(4-{3-[(methylsulfonyl)amino]prop-1-yn-1-yl}phenyl)-4-oxoazetidin-2-yl]phenyl-β-D-glucopyranosiduronic acid (PS) and the alkyl sulfonamide, 4-[(2*S*,3*R*)-3-[(3*S*)-3-(4-fluorophenyl)-3-hydroxypropyl]-1-(4-{3-[(methylsulfonyl)amino]propyl}phenyl)-4-oxoazetidin-2-yl]phenyl β-D-glucopyranosiduronic acid (AS) (Goulet et al., 2005) are named using the IUPAC convention (Fig. 1). All other reagents were obtained from commercial sources and were of the highest purity commercially available.

Preparation of [^{3}H]AS. A solution of PS (2 mg, 0.0028 mmol) in 0.8 ml of anhydrous *N*,*N*-dimethylformamide was degassed at dry ice/acetone temperature in the presence of 5 mg of 10% Pd/C [10% (dry basis) on activated charcoal, wet, Degussa type; Sigma-Aldrich]. The mixture was stirred at 0°C for 2 h under 240 mm Hg of carrier-free tritium gas (1.2 Ci; American Radiolabeled Chemicals, St. Louis, MO). Unreacted tritium gas was removed, the catalyst was filtered

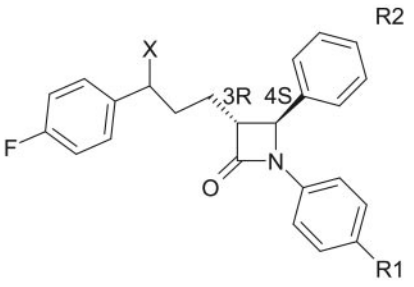

Compound	X	R1	R2
EZE	OH (S)	F	OH
EZE-Gluc	OH (S)	F	
Ent-1	OH (R)	F	
PS	OH (S)		
AS	OH (S)		

Fig. 1. Chemical structure of EZE and select analogs.

through a syringe-less filter device (0.45 μm polytetrafluoroethylene; Autovial; Whatman, Clifton, NJ), and the solvent and labile tritium were removed by concentration to near dryness. This procedure was repeated three times to ensure complete reduction of the C-C triple bonds and ensure high specific activity. The dried residue was resuspended in 2 ml of ethanol and purified by HPLC (HPLC column, 9.4 mm $\times$ 25 cm, CH_3CN:H_2O:trifluoroacetic acid, 25:75:0.1 to 27:73:0.1 in 50 min; Luna Phenyl-Hexyl; Phenomenex, Torrance, CA). The [^{3}H]AS eluted with a retention time of 32 min and was collected as a single fraction (210 mCi; 85 Ci/mmol, radiochemical purity ~99% by HPLC). The identity was confirmed by liquid chromatography/mass spectrometry analysis and HPLC coelution with unlabeled standard.

Cell-Based [^{3}H]AS Binding. rNPC1L1/HEK293 and TsA201 cells were seeded at a density of 10,000 cells per well in 96-well poly-D-lysine–coated plates, and cells were allowed to attach for approximately 18 h at 37°C. TsA201 cells were subsequently transfected with dog NPC1L1/pcDNA5/FRT according to the manufacturer's instructions (Roche) and incubated for 3 days at 37°C. MDCKII-derived, LLC-PKI, HepG2, or CaCo-2 cells were seeded at a density of 25,000 cells per well in 96-well tissue culture-treated plates, and cells were allowed to attach and polarize for approximately 72 h at 37°C, except for CaCo-2 cells, where polarization took approximately 14 days at 37°C. For all binding studies, [^{3}H]AS was added to the well, and cells were incubated under normal growth conditions for determined periods of time. Duplicate samples were averaged for each experimental point. For saturation binding experiments, cells were incubated with increasing concentrations of [^{3}H]AS for 4 h. In competition binding experiments, cells were incubated with [^{3}H]AS in the absence or presence of increasing concentrations of test compound. To determine the kinetics of ligand association, cells were incubated with [^{3}H]AS for different periods of time. Dissociation kinetics were determined by addition of 100 μM EZE-gluc and incubating for different periods of time. Nonspecific binding was defined in the presence of 100 μM EZE-gluc. At the end of the incubation period, cells were washed twice with 200 μl of DMEM to separate bound from free ligand, and radioactivity associated with cells was determined using a β-counter. For acid wash experiments, cells were incubated with either 5 nM (rNPC1L1/HEK293) or 1 nM (MDCKII) [^{3}H]AS for 2 h. Thereafter, plates were placed on ice and cells were washed twice with ice-cold PBS, followed by ice-cold acid wash with DMEM, pH 3.5, for 1, 5, or 15 min. Cells were then washed twice with PBS and re-incubated with [^{3}H]AS for 2 h at 37°C. For Transwell experiments, MDCKII cells were seeded at 200,000 cells/well in a 24-well plate and incubated for 3 days at 37°C. [^{3}H]AS was added to either the apical or basolateral compartment of the Transwell membrane, at a concentration of 1 nM, and incubation took place for 2 h at 37°C. Thereafter, both apical and basolateral compartments were washed three times with PBS, and the transwell filter was cut out and its associated radioactivity determined using a β-counter. Data from saturation, competition and ligand dissociation experiments were analyzed as described previously (Knaus et al., 1995; Priest et al., 2004). The association rate, k_1, was determined by employing the pseudo–first-order rate equation $k_1 = k_{obs}([LR]_e/[L]-[LR]_{max}))$, where $[LR]_e$ is the concentration of the complex at equilibrium, [L] is the concentration of ligand, $[LR]_{max}$ is the total receptor concentration, k_{obs} is the slope of the pseudo–first-order plot, $\ln([LR]_e/([LR]_e - [LR]_t))$ versus time, and $[LR]_t$ is the receptor-ligand complex at one given time point t.

Cloning of Dog NPC1L1 and Expression in MDCKII Cells. Total RNA was isolated from 3×10^7 MDCKII cells using TriReagent and purified with RNeasy columns. Single-stranded cDNA was synthesized from total RNA using SuperScript II and random hexamer primers and subsequently purified with Chromaspin 200 following conditions suggested by the manufacturer (Clontech). BLAST searches of public DNA databases with the human NPC1L1 protein sequence identified a partial sequence for dog NPC1L1. Based on alignments with multiple sequences for NPC1L1, this dog sequence was missing its 3′ region. Using the partial dog NPC1L1 sequence and the human sequence, genomic sequence for dog NPC1L1 was identified. Translation of an open reading frame extracted from the genomic sequence was in good agreement with human and bovine NPC1L1. Therefore, the primers dNL1-sense (CTGCACAGGGATGGCGGACACTGGCCTGAG) and dNL1-antisense (CTCCGGCTTCATCAGAGGTCCGGTCCACTGC) were designed to amplify a product of approximately 4 kilobase pairs using Pfusion DNA polymerase in a high-fidelity PCR reaction performed with single stranded cDNA and an extension time of 135 s and 33 cycles. PCR products from several reactions were combined and purified before cloning into the vector pCDNA5/FRT TOPO. Sequencing of several plasmids containing insert revealed a PCR product for the complete coding region of dog NPC1L1, with start and putative stop codons. Because the insert consistently integrated into pCDNA5/FRT TOPO in the reverse orientation, it was isolated by restriction digest and directionally cloned into the vector pCDNA5/FRT.

MDCKII-Flp cells were generated by stably transfecting with pFRT/lacZeo cDNA (Invitrogen) using Lipofectamine 2000 (Invitrogen) according to manufacturer's instructions. Forty-eight hours after transfection, cells were selected in Zeocin (700 μg/ml), and resulting cell colonies were isolated and assayed for β-galactosidase activity (β-galactosidase assay kit; Invitrogen). The clone with the highest activity was used as the host cell line in subsequent transfections. Dog and human NPC1L1/MDCKII II-Flp stable cell lines were generated by transfecting MDCKII-Flp cells with pCDNA5/FRT-dog NPC1L1 or pCDNA5/FRT-human NPC1L1 plasmids using Lipofectamine, followed by selection on 200 μg/ml Hygromycin B. Clones were isolated with cloning rings and selected for levels of [^{3}H]AS binding in the absence or presence of 10 mM sodium butyrate to identify cells expressing high amounts of human or dog NPC1L1.

RNA Extraction, Reverse Transcription and Quantitative Real-Time PCR. For total RNA isolation and preparation, MDCKII cells were washed once in PBS and immersed in TriReagent. The RNA preparation was performed according to the manufacturer's protocol. In brief, chloroform was added to the cells, and the aqueous phase containing RNA was separated from DNA and protein by centrifugation. The aqueous phase was processed using an RNEasy MicroKit (QIAGEN) yielding pure total RNA and dissolved in water. To allow use of comparable amounts of RNA for cDNA preparation, the RNA concentration in all samples was measured with an Agilent BioAnalyzer 2100 (Agilent Technologies, Palo Alto, CA). Standard reagents (ABI TaqMan reverse transcription reagents; Applied Biosystems) were used to synthesize cDNAs. A maximum of 500 ng of RNA in 100 μl was used for a single reverse transcriptase reaction.

QRT-PCR was conducted using TaqMan technology with oligonucleotide primers and probes custom-ordered from ABI. TaqMan reactions were performed according to standard protocols. Data were analyzed using the standard curve method as described in Applied Biosystems' documentation on Relative Quantitation of Gene Expression for ABI PRISM 7700. The relative expression level of the gene of interest was computed from each experimental sample using a housekeeping gene (18s; Applied Biosystems) as an internal standard. Each experimental sample was quantified in three independent cDNA preparations and repeated at least two times on different plates.

Cell-Based [^{3}H]Cholesterol or [^{3}H]Sitosterol Flux. Flux assays were performed essentially as described by Yu et al. (2006). In brief, cell growth medium was completely aspirated and replaced with 200 μl of 5% lipoprotein-deficient serum (LPDS) containing the appropriate concentration of compound and incubated at 37°C for 3 h in a 5% CO_2 incubator. Media was subsequently aspirated, and cells were incubated in 200 μl of 0 to 5.5% methyl-β-cyclodextrin (βmCD), dissolved in 5% LPDS, and filtered through a 0.22 μM filter, at 37°C for 45 min in a 5% CO_2 incubator. Media was removed and cells were washed twice with 125 μl of 5% LPDS followed by addition of [^{3}H]cholesterol (51 Ci/mmol; PerkinElmer Life and Analytical Sciences, Waltham, MA) or [^{3}H]sitosterol (50 Ci/mmol; American Ra-

diolabeled Chemicals) complexed to bovine serum albumin in 5% LPDS (Yu et al., 2006). After a 45-min incubation, cells were washed twice with DMEM, and 1% SDS was added. Solubilized cell content was transferred to vials for radioactive analyses.

Results

Binding of [^{3}H]AS to Rat NPC1L1 Expressed at the Surface of HEK293 Cells. To determine the surface expression of NPC1L1 in cells, a cell-based assay that quantifies binding of the EZE analog, [^{3}H]AS, to rat NPC1L1 heterologously expressed in HEK293 cells (rNPC1L1/HEK293 cells) was established and validated. When rNPC1L1/HEK293 cells were incubated with increasing concentrations of [^{3}H]AS, in the absence or presence of 100 μM Eze-Gluc, the radioligand associated specifically with cells as a saturable function of ligand concentration and displayed a good signal-to-noise ratio (Fig. 2A). As expected, the nonspecific binding component varied linearly with the [^{3}H]AS concentration. A fit of the specific binding component to a single binding isotherm yielded an equilibrium dissociation constant, K_d, of 4.62 $\pm$ 0.69 nM, and a maximum density of cell surface binding sites, B_{max}, of 180 pM corresponding to 2.21 $\times$ 10^6 binding sites/cell. In comparison, the values of total and nonspecific binding of [^{3}H]AS to nontransfected HEK293 cells were similar to each other and to the nonspecific binding of rNPC1L1/HEK293 cells (Fig. 2A, inset).

Incubation of rNPC1L1/HEK293 cells with 5 nM [^{3}H]AS resulted in a time-dependent association of ligand with cells that reached equilibrium in ~3 h (Fig. 2B). The nonspecific binding component was time-independent and has been subtracted from the experimental data. A semilogarithmic transformation of the data yielded a linear dependence (Fig. 2B, inset), as expected for a pseudo–first-order reaction, and the slope of this line gives k_{obs} of 0.0208 min^{-1}. The association rate constant, k_1, calculated as described under *Materials and Methods*, was 2.4 $\times$ 10^6 M^{-1} min^{-1}. Dissociation of cell bound [^{3}H]AS, initiated by addition of 100 μM Eze-Gluc, followed a single monoexponential decay with a $t_{1/2}$ of ~3 h, corresponding to k_{-1} of 0.0059 min^{-1} (Fig. 2C). The K_d calculated from these rate constants was 2.46 nM, a value similar to that determined under equilibrium binding conditions (4.62 nM). These kinetic observations indicate that [^{3}H]AS bound to a single class of sites through a simple bimolecular and fully reversible reaction.

Binding of [^{3}H]AS to rat NPC1L1/HEK293 cells was inhibited in a concentration-dependent manner by increasing concentrations of AS, PS, EZE-gluc, and EZE (Fig. 2D). K_i values, determined as described under *Materials and Methods*, are presented in Table 1 and display the expected rank-order of potency for interaction of these ligands with rat NPC1L1 (Garcia-Calvo et al., 2005). The EZE-gluc enantiomer ent-1 did not significantly inhibit the binding of [^{3}H]AS to rat NPC1L1/HEK293 cells at concentrations up to 50 μM (Fig. 2D, inset).

To confirm that the noncovalent interaction between [^{3}H]AS and rat NPC1L1 occured at the cell surface, rNPC1L1/HEK293 cells were incubated with [^{3}H]AS and subsequently acid-washed with DMEM at pH 3.5. Such an approach has previously been used to characterize cell-surface noncovalent interactions (Hopkins and Trowbridge, 1983; Chen et al., 1998). Treatment of cells at pH 3.5 for 1, 5, or 15 min led to dissociation of >70, 80, and 85% of bound [^{3}H]AS, respectively (Fig. 2E), indicating that the majority of radioligand binding sites were present at the cell surface and not at intracellular compartments. It is noteworthy that after acid removal, incubation of cells with [^{3}H]AS for 2 h at 37°C causes re-binding of ligand at levels similar to those observed before the acid wash (Fig. 2E), indicating that the loss of radioligand after acid treatment was not due to any significant loss in cell integrity. All data, taken together, strongly indicate that the cell-based binding assay defined cell-surface expression of NPC1L1.

Identification of [^{3}H]AS Binding Activity on the Apical Surface of MDCKII Cells. Because [^{3}H]AS binding to cells can accurately monitor the number of NPC1L1 molecules at the cell surface, two cell lines widely used for studying NPC1L1-dependent processes, CaCo-2 and HepG2, were incubated with [^{3}H]AS to determine whether they specifically bound [^{3}H]AS (Fig. 3A). Under the growth and assay conditions described under *Materials and Methods* for CaCo-2 and HepG2 cells, specific binding of [^{3}H]AS was not observed in any case at ligand concentrations of up to 100 nM (data not shown). Applying a consistent difference of approximately 200 cpm as our limit of detection, these observations indicate that the number of surface [^{3}H]AS binding sites in CaCo-2 and HepG2 would have to be below 5 $\times$ 10^4 sites/cell. In contrast, analysis of the polarized, kidney-derived cell line MDCKII demonstrated specific [^{3}H]AS binding, whereas LLC-PK1 cells, another kidney-derived cell line, displayed no detectable levels of [^{3}H]AS binding (Fig. 3A). Binding of [^{3}H]AS to MDCKII cells was further characterized with saturation binding studies, indicating that [^{3}H]AS binding to MDCKII cells occurred in a concentration-dependent and saturable manner to a single class of sites that displayed a K_d of 0.59 $\pm$ 0.07 nM and a B_{max} of 87 pM, corresponding to 4.19 $\times$ 10^5 sites/cell (Fig. 3B).

The kinetics of [^{3}H]AS binding to MDCKII cells demonstrated that radioligand binding occurred through a simple bimolecular reaction. Thus, incubation of MDCKII cells with [^{3}H]AS results in a time-dependent association of ligand with cells that reached equilibrium in ~2 h. A semilogarithmic transformation of the data yielded a linear dependence, as expected for a pseudo–first-order reaction, and the slope of this line gives a k_{obs} value of 0.0247 min^{-1} (Fig. 4A), from which k_1 of 1.63 $\times$ 10^7 $M^{-1}min^{-1}$ could be calculated. Dissociation of cell-bound [^{3}H]AS, initiated by addition of 100 μM Eze-Gluc, followed a single monoexponential decay with a $t_{1/2}$ of ~3 h, corresponding to k_{-1} of 0.0023 min^{-1} (Fig. 4B). The K_d calculated from these rate constants, 0.14 pM, was similar to that determined under equilibrium binding conditions, 0.59 $\pm$ 0.07 nM, (Fig. 3B).

As previously observed with rNPC1L1/HEK293 cells, acid washing of MDCKII cells equilibrated with [^{3}H]AS leads to dissociation of up to 85% of the radioligand (Fig. 4C). Likewise, after acid removal, [^{3}H]AS bound to MDCKII cells at levels similar to those obtained before acid treatment, indicating that the loss of binding was due not to any significant loss in cell integrity but to disruption of noncovalent interactions between ligand and cell surface expressed NPC1L1-like activity.

Because MDCKII cells, like enterocytes and hepatocytes, are polarized epithelial cells demonstrating microvilli and tight junctions, the distribution of [^{3}H]AS binding sites was evaluated on Transwell supports, where cells polarize to form an impermeable barrier between the apical and basolateral

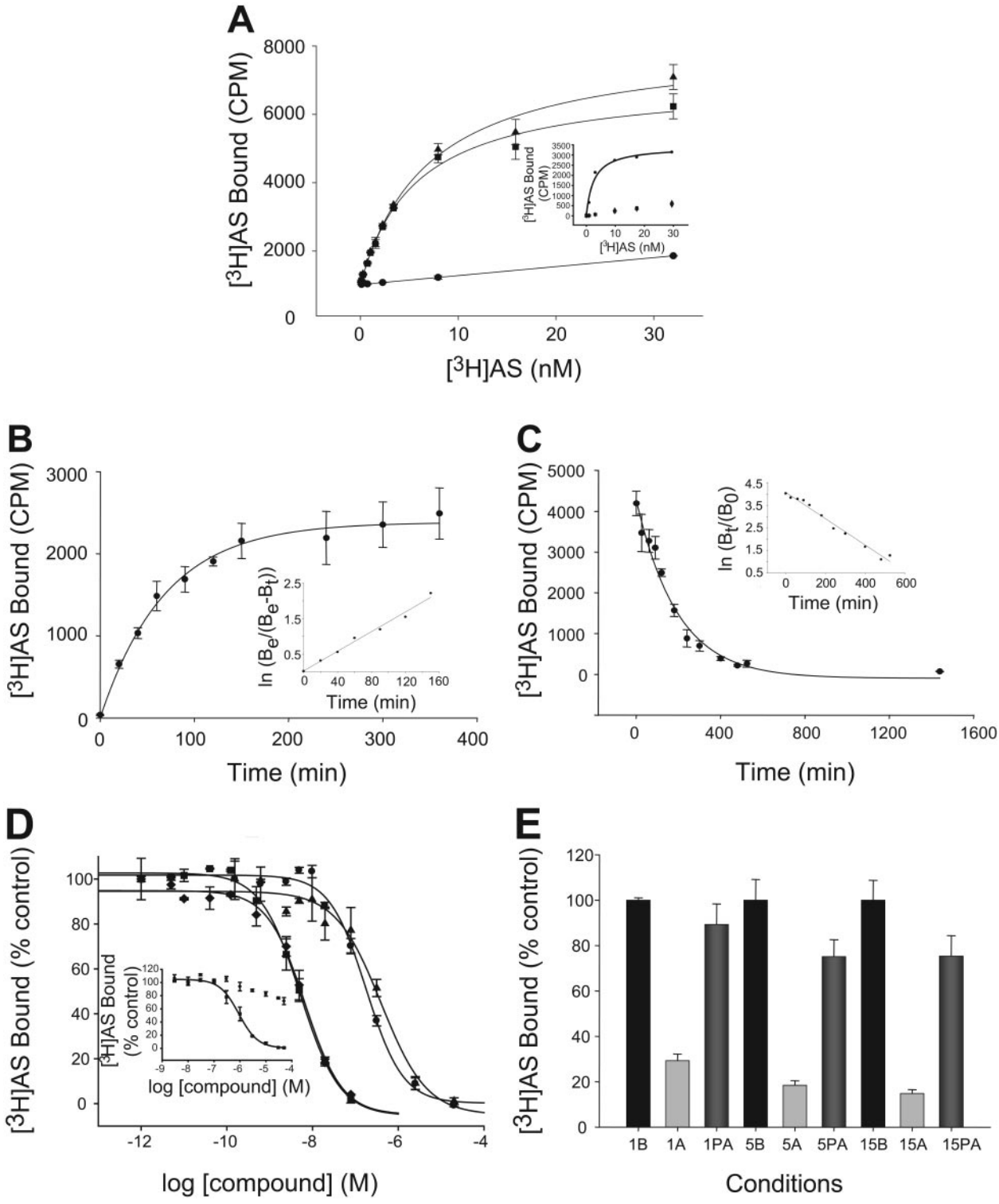

Fig. 2. Binding of [^{3}H]AS to rNPC1L1/HEK293 cells. A, saturation studies. rNPC1L1/HEK293 cells were seeded in 96-well poly-D-lysine plates at a density of 10,000 cells/well and incubated with increasing concentrations of [^{3}H]AS for 4 h at 37°C. Separation of bound from free radioligand was carried out as indicated under *Materials and Methods*. Total binding (▲), nonspecific binding determined in the presence of 100 μM EZE-gluc (●), and specific binding (■), defined as the difference between total and nonspecific binding are presented. Specific binding was a saturable function of [^{3}H]AS concentration and displayed a single high-affinity site with K_d of 4.62 nM and B_{max} of 2.21×10^6 sites/cell. Inset, saturation studies of HEK293 and rNPC1L1/HEK293 cells. Saturation studies were performed as described above. Total (●) and nonspecific (■) binding to rNPC1L1/HEK293 and HEK293 cells [Total (▲) and nonspecific binding (▼)] are presented. B, association kinetics. rNPC1L1/HEK293 cells were incubated with 5 nM [^{3}H]AS for indicated amounts of time at 37°C. Nonspecific binding determined in the presence of 100 μM EZE-gluc was time invariant and has been subtracted from experimental points. Inset, a semilogarithmic representation of the pseudo–first-order association reaction, where B_e and B_t represent ligand bound at equilibrium (e) and time t, respectively, yielded k_{obs} (0.0208 min^{-1}), corresponding to a k_1 of 0.0024 nM^{-1} min^{-1}. C, dissociation kinetics. After incubation with 5 nM [^{3}H]AS overnight, wells were rinsed and rNPC1L1/HEK293 cells were incubated with growth media containing 100 μM Eze-Gluc for different amounts of time at 37°C. [^{3}H]AS dissociation followed monoexponential kinetics, indicative of a first-order reaction with k_{-1} = 0.0059 min^{-1}. The K_d determined from k_{-1}/k_1 is 2.46 nM. D, pharmacology. rNPC1L1/HEK293 cells were incubated with 5.36 nM [^{3}H]AS in the

compartments. Addition of 1 nM [^{3}H]AS to the apical side of the Transwell, which represents the apical surface of MDCKII cells, led to significant specific [^{3}H]AS binding (Fig. 4D). However, when the same amount of ligand was added to the basolateral side of the Transwell, corresponding to the basolateral surface of the MDCKII cells, specific [^{3}H]AS binding was significantly lower than in the previous situation (Fig. 4D), indicating that most of the NPC1L1-like activity resided at the apical surface of MDCKII cells. Furthermore, these results suggest that [^{3}H]AS did not appreciably diffuse through the membrane, into the cell, because in such a case, it should have been able to reach [^{3}H]AS binding sites, regardless of their apical or basolateral localization.

The NPC1L1-like activity expressed at the apical surface of MDCKII cells was further characterized pharmacologically using a series of EZE-like compounds (Fig. 4E and Table 1). Similarly to rat NPC1L1 expressed in HEK293 cells, AS and PS displayed equivalent potency as inhibitors of [^{3}H]AS binding to MDCKII cells [K_i values of 0.34 ± 0.04 nM (AS) and 0.33 ± 0.05 nM (PS)], EZE-gluc being ~10-fold weaker (K_i of 3.51 ± 0.89 nM) and EZE being the weakest of all tested analogs (K_i of 14.01 ± 4.11 nM). It is worth noting that although the relative potencies of these compounds are similar for rat NPC1L1 expressed in HEK293 cells and MDCKII cells, the absolute affinities are higher for MDCKII cells.

Cloning and Pharmacological Characterization of the NPC1L1-Like Activity from MDCKII Cells. Given that [^{3}H]AS binding data strongly suggest the presence of NPC1L1 in the apical membrane of MDCKII cells, total RNA was isolated from MDCKII cells, and a full-length clone containing a single amino acid change from the predicted dog NPC1L1 genomic sequence (I864M) was isolated. This clone is in agreement with another recently reported dog NPC1L1 sequence (Hawes et al., 2007) with the exception of a single amino acid change (L63P). Dog NPC1L1, like its homologs in other species, was predicted to have 13 transmembrane domains, the *N* terminus being extracellular and the C terminus, intracellular. Likewise, the sterol-sensing domain was conserved with that found in other species. These data strongly suggest that the NPC1L1-like activity from MDCKII cells indeed represents dog NPC1L1 and is consistent with all the features of [^{3}H]AS interaction with these cells.

To further validate this idea, cloned dog NPC1L1 was transiently expressed in TsA201 cells, and binding of [^{3}H]AS

TABLE 1

Binding properties of select β-lactams to rat NPC1L1/HEK293, MDCKII cells, or dog NPC1L1 transiently expressed in TsA201 cells

K_d values were determined from saturation experiments using increasing concentrations of [^{3}H]AS. Values represent the mean ± S.D. of at least three independent determinations, as described under *Materials and Methods*. K_i values were determined from competition experiments using [^{3}H]AS and increasing concentrations of unlabeled β-lactams. Values represent the mean ± S.D. of two to six independent determinations.

	rNPC1L1/HEK293	MDCKII	Dog NPC1L1/TsA 201
	nM	*nM*	*nM*
K_d (AS)	4.62 ± 0.69	0.59 ± 0.07	0.52 ± 0.05
K_i (AS)	2.35 ± 0.49	0.34 ± 0.04	0.47 ± 0.11
K_i (PS)	4.07 ± 1.47	0.33 ± 0.05	N.D.
K_i (EZE)	209 ± 40.4	14.01 ± 4.11	N.D.
K_i (EZE-gluc)	95.1 ± 8.62	3.51 ± 0.89	5.91 ± 1.52

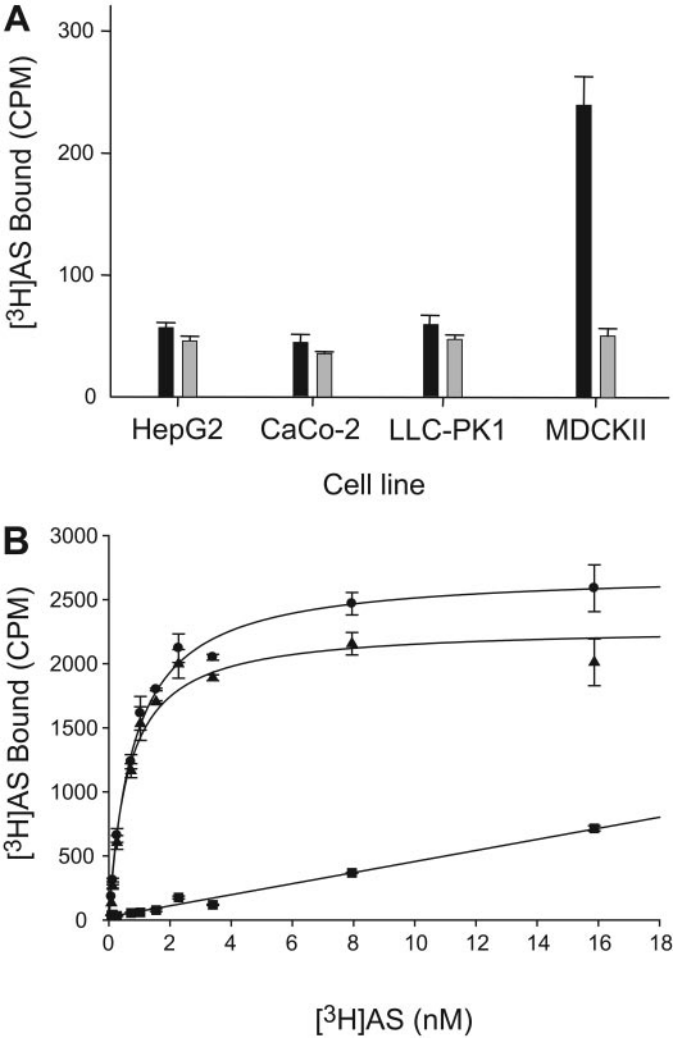

Fig. 3. MDCKII cells possess a robust NPC1L1-like [^{3}H]AS binding activity. A, [^{3}H]AS binding to selected cell lines. At the appropriate time after seeding, cells were incubated with 5 nM [^{3}H]AS at 37°C for 4 h in the absence or presence of 100 μM EZE-gluc. B, binding to MDCKII cells. MDCKII cells were seeded into tissue culture-treated, white-walled 96-well plates at a density of 25,000 cells/well and incubated with increasing concentrations of [^{3}H]AS for 4 h at 37°C. Separation of bound from free radioligand was carried out as indicated under *Materials and Methods*. Total binding (●), nonspecific binding determined in the presence of 100 μM EZE-gluc (■) and specific binding (▲), defined as the difference between total and nonspecific binding, are presented. Specific binding was a saturable function of [^{3}H]AS concentration and displayed a single high-affinity site with K_d of 0.59 nM and B_{max} of 4.19 × 10^5 sites/cell.

presence or absence of increasing concentrations of AS (■), PS (♦), EZE-gluc (●), or EZE (▲) for 4 h at 37°C. Inhibition of binding was assessed relative to an untreated control. Specific binding was fit to a single-site inhibition model, yielding IC_{50} values of 5.25 nM (AS) (■), 6.61 nM (PS) (♦), 398 nM (EZE) (▲), and 182 nM (EZE-gluc) (●). Inset, pharmacology. rNPC1L1/HEK293 cells were incubated with 10.82 nM [^{3}H]AS in the presence or absence of increasing concentrations of EZE (■) or ent-1 (●) for 4 h at 37°C. Inhibition of binding was assessed relative to an untreated control. Specific binding was fit to a single-site inhibition model, yielding IC_{50} values of 912 nM (EZE) (■) and N.D. (ent-1) (●). E, acid wash. rNPC1L1/HEK293 cells were incubated with 5 nM [^{3}H] AS (1B, 5B, 15B). After washing the cells once with PBS, the cells were acid-washed by incubation in DMEM, pH 3.5, for 1 (1A), 5 (5A), or 15 min (15A). Thereafter, acid was removed by two PBS washes, and cells were incubated for 2 h with 5 nM [^{3}H]AS (1PA, 5PA, 15PA). Specific binding in each case is presented relative to an untreated control.

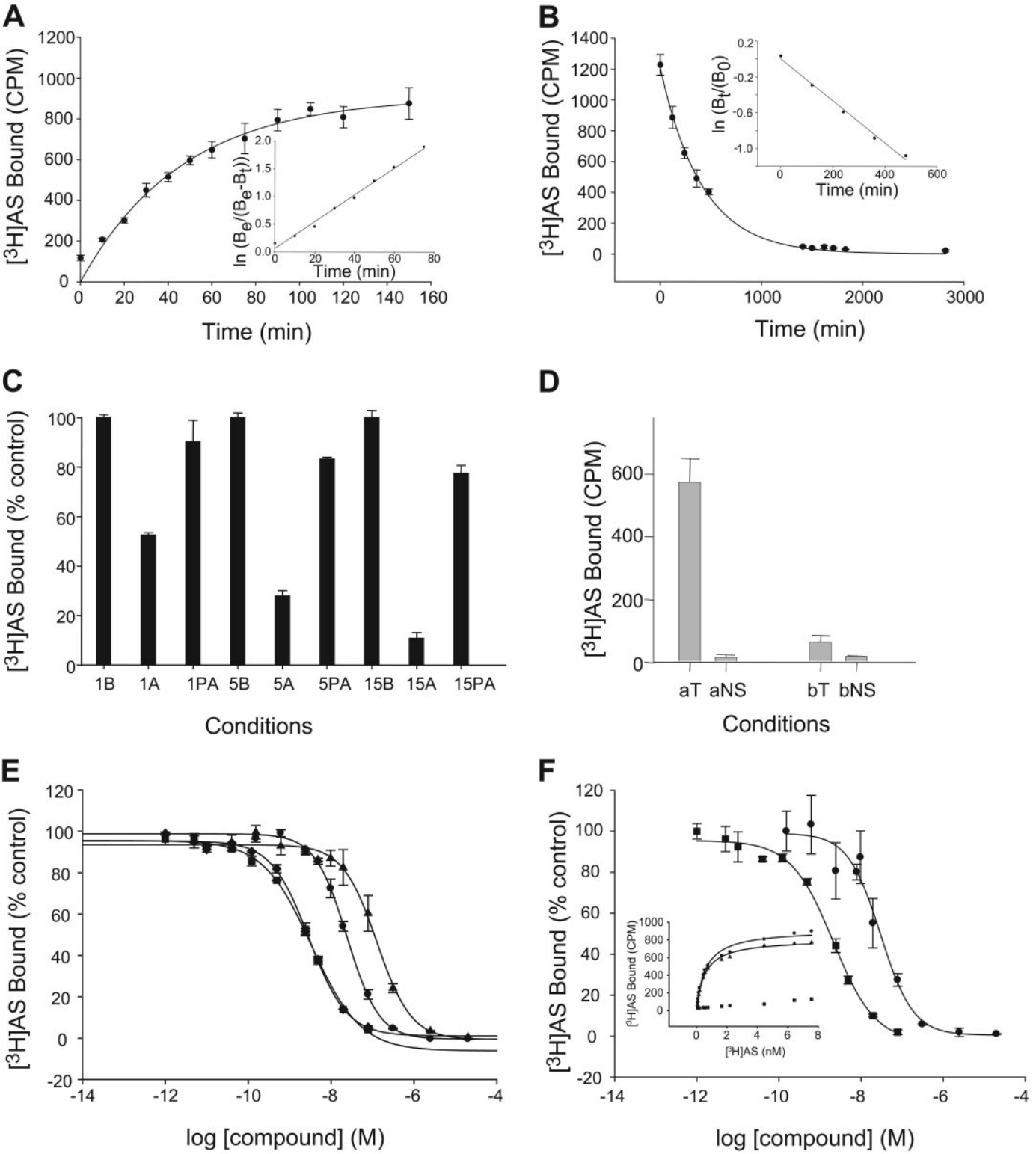

Fig. 4. Binding to MDCKII cells and transiently transfected TsA201 cells. A, association kinetics. Cells were incubated with 1.2 nM [^{3}H]AS for indicated amounts of time at 37°C. Nonspecific binding determined in the presence of 100 μM EZE-gluc was time-invariant and has been subtracted from experimental points. Inset, a semilogarithmic representation of the pseudo–first-order association reaction, where B_e and B_t represent ligand bound at equilibrium (e) and time t, respectively, yielded k_{obs} (0.0247 min^{-1}), corresponding to a k_1 of 0.0163 nM^{-1} min^{-1}. B, dissociation kinetics. After incubation with 1 nM [^{3}H]AS overnight, wells were rinsed and cells were incubated with growth media containing 100 μM Eze-Gluc for different amounts of time at 37°C. [^{3}H]AS dissociation followed monoexponential kinetics, indicative of a first-order reaction with k_{-1} = 0.0023 min^{-1}. The K_d determined from k_{-1}/k_1 is 0.14 nM. C, acid wash of [^{3}H]AS bound to MDCKII cells. MDCKII cells were incubated with 5 nM [^{3}H]AS for 2 h (1B, 5B, 15B). After washing the cells once with PBS, cells were acid-washed by incubation in DMEM, pH 3.5, for 1 (1A), 5 (5A), or 15 min (15A). Thereafter, acid was removed by two PBS washes and cells were incubated with 5 nM [^{3}H]AS for 2 h (1PA, 5PA, 15PA). Specific binding data are presented relative to an untreated control. D, NPC1L1-like activity is expressed at the apical membrane of MDCKII cells. MDCKII cells were incubated with 1 nM [^{3}H]AS added to either the apical (a) or basolateral (b) side of cells grown on impermeable Transwells in the absence (T) or presence (NS) of 100 μM EZE-gluc.

to these cells was then characterized (Fig. 4F and Table 1). Under equilibrium binding conditions, [^{3}H]AS bound with a K_d of 0.52 ± 0.05 nM and a B_{max} of approximately 2 × 10^5 sites/cell (Table 1 and Fig. 4F, inset). Furthermore, AS and EZE-gluc inhibited [^{3}H]AS binding to dog NPC1L1 transiently expressed in TsA201 cells with K_i values of 0.47 ± 0.11 and 5.91 ± 0.08, respectively (Fig. 4F), in agreement with the K_d and K_i values obtained for [^{3}H]AS binding to MDCKII cells. Thus, the data are consistent with the endogenous expression of dog NPC1L1 in MDCKII cells.

Surface Expression of NPC1L1 in MDCKII Cells Is Sensitive to Cell Cholesterol Levels. To determine whether the surface expression of NPC1L1 in MDCKII cells was sensitive to changes in the endogenous concentration of cholesterol, MDCKII cells were seeded and grown in either 10% FBS or 5% LPDS in the absence or presence of the HMG CoA reductase inhibitor lovastatin. MDCKII cells grown in either 10% FBS or 5% LPDS displayed an increase in the amount of [^{3}H]AS binding up to 72 h (Fig. 5A, I and II). Incubation of MDCKII cells with 4 μM lovastatin and 10% FBS led to a 40% increase in the surface expression of NPC1L1 at the 72-h time point (Fig. 5A, I). In contrast, lovastatin treatment tripled [^{3}H]AS binding in cells grown in 5% LPDS at 72 h (Fig. 5A, II). The increase in [^{3}H]AS binding caused by lovastatin/5% LPDS was due not to enhanced [^{3}H]AS affinity (K_d values of 180 nM in either case) but to an increase in the number of NPC1L1 sites at the cell surface [B_{max} of 75 pM (5% LPDS) and 154 pM (5% LPDS and 4 μM lovastatin)] (Fig. 5B).

To gain insight into the mechanism underlying the lovastatin-induced increase in [^{3}H]AS binding to cells grown in 5% LPDS, we determined the amount of NPC1L1 and HMG CoA reductase message by QRT-PCR. QRT-PCR indicated that 4 μM lovastatin led to an increase in the amount of HMG CoA reductase transcript in MDCKII cells grown in either 10% FBS or 5% LPDS (Fig. 5C, I and II). Furthermore, over time, QRT-PCR demonstrated that the amount of dog NPC1L1 transcript increased in MDCKII cells grown in either 10% FBS or 5% LPDS (Fig. 5C, III and IV). However, when MDCKII cells were grown in 10% FBS, 4 μM lovastatin did not increase transcription of dog NPC1L1 above that observed in untreated cells (Fig. 5C, III). In contrast, when MDCKII cells were grown in 5% LPDS, 4 μM lovastatin increased dog NPC1L1 transcription above that observed in untreated cells (Fig. 5C, IV).

Overexpression of NPC1L1 in MDCKII-Flp cells Was Necessary for EZE-Like-Sensitive [^{3}H]Cholesterol Flux. To validate MDCKII cells as an appropriate surrogate system for monitoring NPC1L1-dependent processes, we evaluated their ability to perform EZE-sensitive cholesterol flux using a protocol similar to that reported recently (Yu et al., 2006). This assay makes use of the ability of βmCD to deplete membrane-bound cholesterol. Subsequent exposure of cells to [^{3}H]cholesterol provided a time-dependent flux of this substrate into the cells. However, pretreatment of MDCKII-Flp cells with 4% βmCD caused only a small increase in [^{3}H]cholesterol influx into the cells that was marginally blocked by 10 μM PS (Fig. 6A, I). In an attempt to improve the assay window, we generated hNPC1L1/MDCKII-Flp, a stable MDCKII-Flp cell line overexpressing human NPC1L1. [^{3}H]AS binding to MDCKII-Flp or hNPC1L1/MDCKII-Flp cells indicated that the expression of human NPC1L1 led to a change in K_d from 0.4 to 11 nM as a consequence of the dramatic increase in levels of hNPC1L1; B_{max} increased from 73 pM (3.55 × 10^5 sites/cell) in MDCKII-Flp cells to 1260 pM (6.07 × 10^6 sites/cell) in hNPC1L1/MDCKII-Flp cells (Fig. 6A, II). It is noteworthy that in hNPC1L1/MDCKII-Flp cells, treatment with 4% βmCD led to a significant increase in the amount of [^{3}H]cholesterol influx into cells that was almost completely blocked in the presence of 10 μM PS (Fig. 6A, III). Addition of 4 mM sodium butyrate (Chen et al., 1997) had no significant effect on the amount of [^{3}H]cholesterol influx into either MDCKII or hNPC1L1/MDCKII-Flp cells or the block by 10 μM PS (Fig. 6A, I and III, inset).

Further evidence for the role of NPC1L1 expression levels on EZE-sensitive [^{3}H]cholesterol influx was obtained by analyzing the properties of MDCKII-Flp cells overexpressing dog NPC1L1 (dNPC1L1/MDCKII-Flp cells) in an inducible manner. Without induction, dNPC1L1/MDCKII-Flp cells bound [^{3}H]AS with a K_d of 0.78 nM and a B_{max} of 131 pM (6.23 × 10^5 sites/cell, Fig. 6B, II), and treatment of the cells with 4% βmCD did not significantly increase the amount of [^{3}H]cholesterol entering cells in an EZE-sensitive manner (Fig. 6B, I). After induction of dNPC1L1/MDCKII-Flp cells for 24 h with 4 mM sodium butyrate (Chen et al., 1997), K_d remained similar at 1.53 nM; however, the B_{max} rose to 384 pM (1.83 × 10^6 sites/cell; Fig. 6B, II). It is noteworthy that after NPC1L1 induction, treatment of the cells with 4% βmCD led to a significant increase in the amount of [^{3}H]cholesterol entering cells, and this process was almost completely blocked by 10 μM PS (Fig. 6B, III).

Relationship between EZE Analog Binding to NPC1L1 and Reduction in Cholesterol and Sitosterol Flux. To further understand the [^{3}H]cholesterol influx process into MDCKII cells, the potency of the EZE-like compound PS for inhibiting [^{3}H]cholesterol uptake was determined. [^{3}H]Cholesterol influx into both dNPC1L1/MDCKII-Flp and human NPC1L1/MDCKII-Flp cells was found to be sensitive to the presence of increasing concentrations of PS. IC_{50} values for inhibition of [^{3}H] cholesterol uptake [10.3 ± 1.5 and 0.32 ± 0.09 nM for hNPC1L1/MDCKII-Flp and dNPC1L1/MDCKII-Flp, respectively (Fig. 7A, I and II)] correlated well with corresponding binding K_d values, 11 and 0.8 nM. In addition, in agreement with a previous report (Yamanashi et al., 2007), [^{3}H]sitosterol behaved in a manner similar to that [^{3}H]cholesterol in both

E, pharmacology of [^{3}H]AS binding to MDCKII cells. Cells were incubated with 5.49 nM [^{3}H]AS in the presence or absence of increasing concentrations of AS (■), PS (♦), EZE-gluc (●), or EZE (▲) for 4 h at 37°C. Inhibition of binding was assessed relative to an untreated control. Specific binding was fit to a single-site inhibition model, yielding IC_{50} values of 2.86 nM (AS) (■), 3.02 nM (PS) (♦), 126 nM (EZE) (▲), and 24 nM (EZE-gluc) (●). F, pharmacology of [^{3}H]AS binding to cloned dog NPC1L1 cDNA expressed in TsA201 cells. TsA201 cells transiently transfected with dog NPC1L1 cDNA were incubated with 1.64 nM [^{3}H]AS in the presence or absence of increasing concentrations of AS (■) or EZE-gluc (●) for 4 h at 37°C. Inhibition of binding was assessed relative to an untreated control. Specific binding was fit to a single-site inhibition model, yielding IC_{50} values of 2 nM (AS) (■) and 26 nM (EZE-gluc) (●). Inset, saturation binding to cloned dog NPC1L1 expressed in TsA201 cells. TsA201 cells transiently transfected with dog NPC1L1 cDNA were incubated with increasing concentrations of [^{3}H]AS for 4 h at 37°C. Separation of bound from free radioligand was carried out as indicated under *Materials and Methods*. Total binding (●), nonspecific binding determined in the presence of 100 μM EZE-gluc (■), and specific binding (▲), defined as the difference between total and nonspecific binding, are presented. Specific binding was a saturable function of [^{3}H]AS concentration and displayed a single high-affinity site with K_d of 0.57 nM and B_{max} of 2 × 10^5 sites/cell.

dNPC1L1/MDCKII-Flp and hNPC1L1/MDCKII-Flp cells with IC_{50} values for inhibition of [^{3}H] sitosterol uptake of 5 ± 1.5 and 0.8 ± 0.09 nM for hNPC1L1/MDCKII-Flp and dNPC1L1/MDCKII-Flp, respectively (Fig. 7A, III and IV), correlating well with corresponding K_d values for [^{3}H]AS and IC_{50} values for [^{3}H]cholesterol.

Furthermore, the rank order of potency for a series of β-lactams as inhibitors of [^{3}H]AS binding (Fig. 7B, I) [PS (5 nM)≫EZE-gluc (209 nM)≫ent-1 (N.D., > 100 μM)] correlates well with the IC_{50} values of these compounds for blocking [^{3}H]cholesterol influx (Fig. 7B, II) [PS (7 nM)≫EZE-Gluc (300 nM)≫ ent-1 (N.D., > 100 μM)] into hNPC1L1/MDCKII-Flp cells. These data, taken together, strongly support the notion that MDCKII cells represent a powerful functional system for studying NPC1L1-dependent processes and provide insight into the mechanism of EZE inhibition of cholesterol flux.

Discussion

To understand the molecular mechanism of EZE-sensitive NPC1L1 dependent cholesterol flux in vitro, researchers

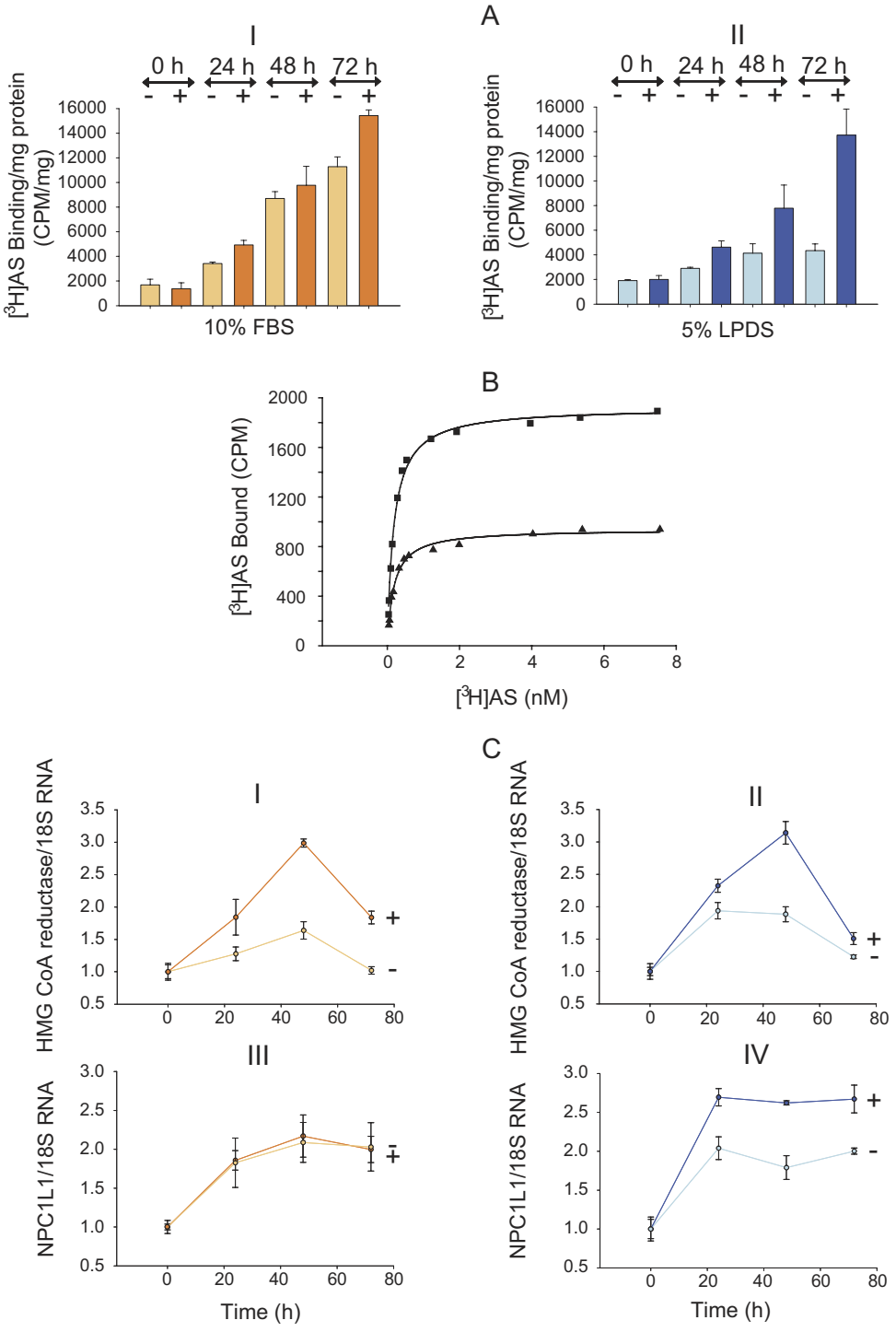

Fig. 5. Blocking endogenous cholesterol synthesis in MDCKII cells leads to an increase in [^{3}H]AS binding. A, time course of 5 nM [^{3}H]AS binding to MDCKII cells grown in either 10% FBS (I) or 5% LPDS (II) in the absence (−) or presence (+) of 4 μM lovastatin. At each time point, cells were harvested and [^{3}H]AS binding determined in the absence (T) or presence (NSB) of 100 μM EZE-gluc, as described previously. Specific [^{3}H]AS binding under each experimental condition are plotted. B, lovastatin leads to an increase in [^{3}H]AS binding to MDCKII cells grown in 5% LPDS. Saturation binding of [^{3}H]AS to MDCKII cells 3 days after initiating growth in either 5% LPDS (▲) or 5% LPDS with 4 μM lovastatin (■). Binding was measured with 25,000 cells in a volume of 200 μl after 2 h incubation at 37°C. Specific binding data were fit by nonlinear regression as described under *Materials and Methods*, to identify a single high-affinity site with K_d = 180 pM and B_{max} of either 75 pM [5% LPDS (▲)] or 154 pM [5% LPDS and 4 μM lovastatin (■)]. C, QRT-PCR analysis of HMG CoA reductase (I and II) and NPC1L1 (III and IV) expression in MDCKII cells grown in 10% FBS (I and III) or 5% LPDS (II and IV) with (+) or without (−) 4 μM lovastatin. Data were normalized using the housekeeping gene 18S. Data are expressed as mean ± S.D. of relative mRNA quantity.

have developed surrogate cell lines for the enterocyte that have been characterized either on the basis of NPC1L1 localization [using fusion to fluorescent proteins (Davies et al., 2005; Yu et al., 2006; Brown et al., 2007), immunocytochemistry (Davies et al., 2005), cell-surface biotinylation (Davies et al., 2005) or immunoblotting (Iyer et al., 2005; Sané et al., 2006)] or functional assay [EZE-sensitive [^{3}H]Ch flux (Sané et al., 2006; Yu et al., 2006; Field et al., 2007; Yamanashi et al., 2007) or effects on transcripts after siRNA reduction of NPC1L1 expression (Sané et al., 2006)]. Here, we reasoned that an appropriate cell line for studying NPC1L1-dependent processes will express NPC1L1 at the cell surface for interaction with EZE-like compounds. To identify such a system, a cell-based binding assay that allows the quantitative anal-

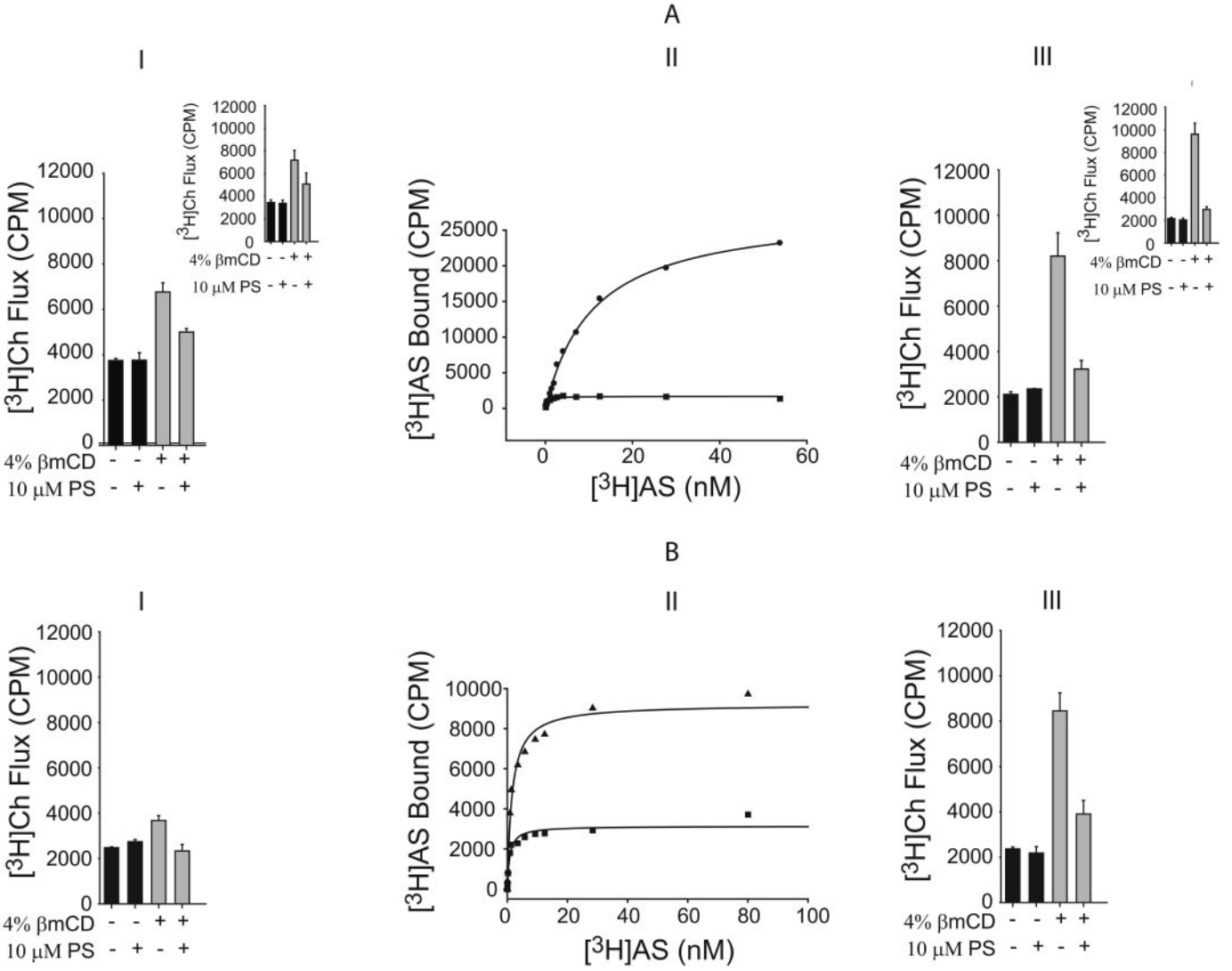

Fig. 6. Development of a functional assay for [^{3}H] sterol influx into MDCKII-Flp cells overexpressing dog or human NPC1L1. A, correlation of human NPC1L1 expression levels with PS blockable [^{3}H]cholesterol influx into MDCKII-Flp cells and human NPC1L1 variants. I, effect of βmCD and PS on influx of [^{3}H]Ch into MDCKII-Flp cells. Cells were seeded on 96-well plates and [^{3}H]Ch flux was performed as described under *Materials and Methods*. Cells were preincubated in the absence or presence of 10 μM PS for 3 h. Thereafter, cells were incubated with or without 4% βmCD for 45 min before addition of [^{3}H]cholesterol in 5% LPDS. Inset, effect of 24-h incubation in 4 mM NaBut on I. II, binding of [^{3}H]AS to MDCKII-Flp and human NPC1L1/MDCKII II-Flp cells. MDCKII-Flp (■) and hNPC1L1/MDCKII-Flp (●) cells were seeded on 96-well plates and incubated with increasing concentrations of [^{3}H]AS for 4 h at 37°C. Specific binding was fit to a single-site saturation model, yielding K_d/B_{max} values of 0.4 nM/73 pM for MDCKII-Flp cells (■) and 11 nM/1260 pM for hNPC1L1/MDCKII-Flp cells (●). III, effect of βmCD and PS on influx of [^{3}H]Ch into human NPC1L1/MDCKII-Flp cells. Cells were seeded on 96-well plates and [^{3}H]Ch flux was performed as described under *Materials and Methods*. Cells were preincubated in the absence or presence of 10 μM PS for 3 h. Thereafter, cells were incubated with or without 4% βmCD for 45 min before addition of [^{3}H]cholesterol in 5% LPDS. Inset, effect of 24-h incubation in 4 mM NaBut on III. B, correlation of dog NPC1L1 expression levels with PS blockable [^{3}H]cholesterol influx into MDCKII-Flp cells and dog variants. I, effect of βmCD and PS on influx of [^{3}H]Ch into dNPC1L1/MDCKII-Flp cells. Cells were seeded on 96-well plates and [^{3}H]Ch flux was performed as described under *Materials and Methods*. Cells were preincubated in the absence or presence of 10 μM PS for 3 h. Thereafter, cells were incubated with or without 4% βmCD for 45 min before addition of [^{3}H]cholesterol in 5% LPDS. II, binding of [^{3}H]AS to dog NPC1L1/MDCKII II-Flp cells before and after induction with sodium butyrate. Dog NPC1L1/MDCKII-Flp cells before (■) or after treatment with 4 mM sodium butyrate (▲) were seeded on 96-well plates and incubated with increasing concentrations of [^{3}H]AS for 4 h at 37°C. Specific binding was fit to a single-site saturation model, yielding K_d/B_{max} values of 0.78 nM/131 pM for control dNPC1L1/MDCKII-Flp cells (■) and 1.53 nM/ 384 pM for cells after 24 h induction with 4 mM sodium butyrate (▲). III, effect of βmCD and PS on influx of [^{3}H]Ch into dog NPC1L1/MDCKII-Flp cells. Cells were seeded on 96-well plates, dog NPC1L1 was induced for 24 h with 4 mM sodium butyrate, and [^{3}H]Ch flux was performed as described under *Materials and Methods*. Cells were preincubated in the absence or presence of 10 μM PS for 3 h. Thereafter, cells were incubated with or without 4% βmCD for 45 min before addition of [^{3}H]cholesterol in 5% LPDS.

ysis of surface NPC1L1 interaction with the high-affinity EZE-like radioligand, [^{3}H]AS, was developed using rNPC1L1/HEK293 cells.

Using high-affinity radiolabeled [^{3}H]AS, we present three lines of evidence indicating that the cell-based binding assay measures [^{3}H]AS bound to rat NPC1L1 at the plasma membrane of rNPC1L1/HEK293 cells. First, the relatively slow association of radioligand exhibits monoexponential kinetics, indicating that binding occurs to a single class of NPC1L1 binding sites. Given the extremely low background of radioligand binding to untransfected HEK293 cells and the hydrophilic properties of the glucuronide moiety, it is unlikely that [^{3}H]AS would passively diffuse across the plasma membrane to bind to a single population of intracellular NPC1L1 sites. Second, dissociation of radioligand is almost complete and exhibits monoexponential kinetics, consistent with release from a single pool of binding sites. Third, acid washing of cells discriminates between noncovalent interactions occurring at the cell surface or inside the cell. The ability to wash off $>$ 75% of bound radioligand with a 1 min of acid treatment and its subsequently rebinding after acid removal supports the contention that the cell-based binding assay measures the cell surface interaction between NPC1L1 and EZE-like compounds (Hopkins and Trowbridge, 1983). These studies extend a recent report documenting the use of a fluorescent EZE analog to monitor equilibrium binding to various species of NPC1L1 expressed in cells (Hawes et al., 2007).

We used binding of [^{3}H]AS to explore surface expression of NPC1L1 in the widely used CaCo-2 (Davies et al., 2005; During et al., 2005; Garmy et al., 2005; van der Veen et al., 2005; Duval et al., 2006; Sané et al., 2006; Alrefai et al., 2007; Field et al., 2007; Mathur et al., 2007; Yamanashi et al., 2007) and HepG2 (Davies et al., 2005; Yu et al., 2006) cells. However, we found that under basal conditions, there was not detectable surface expression of NPC1L1 in these cell lines. Such low surface expression of NPC1L1 is consistent with reports indicating that the majority of NPC1L1 is expressed intracellularly under basal conditions (Davies et al., 2005; Yu et al., 2006). Based on the lower limit of sensitivity of our assay, we speculate that the endogenous expression of NPC1L1 in the apical membrane of CaCo-2 cells (Sané et al., 2006) must be low ($<5 \times 10^4$[^{3}H]AS sites/cell). Critically, exploiting [^{3}H]AS to define surface NPC1L1 expression will allow the in vitro relationship between subcellular localization of NPC1L1 and EZE-effects on NPC1L1-dependent processes to be quantitatively explored across cell systems.

In contrast to CaCo-2 and HepG2 cells, the cell-based radioligand binding assay identified polarized, epithelial MD-

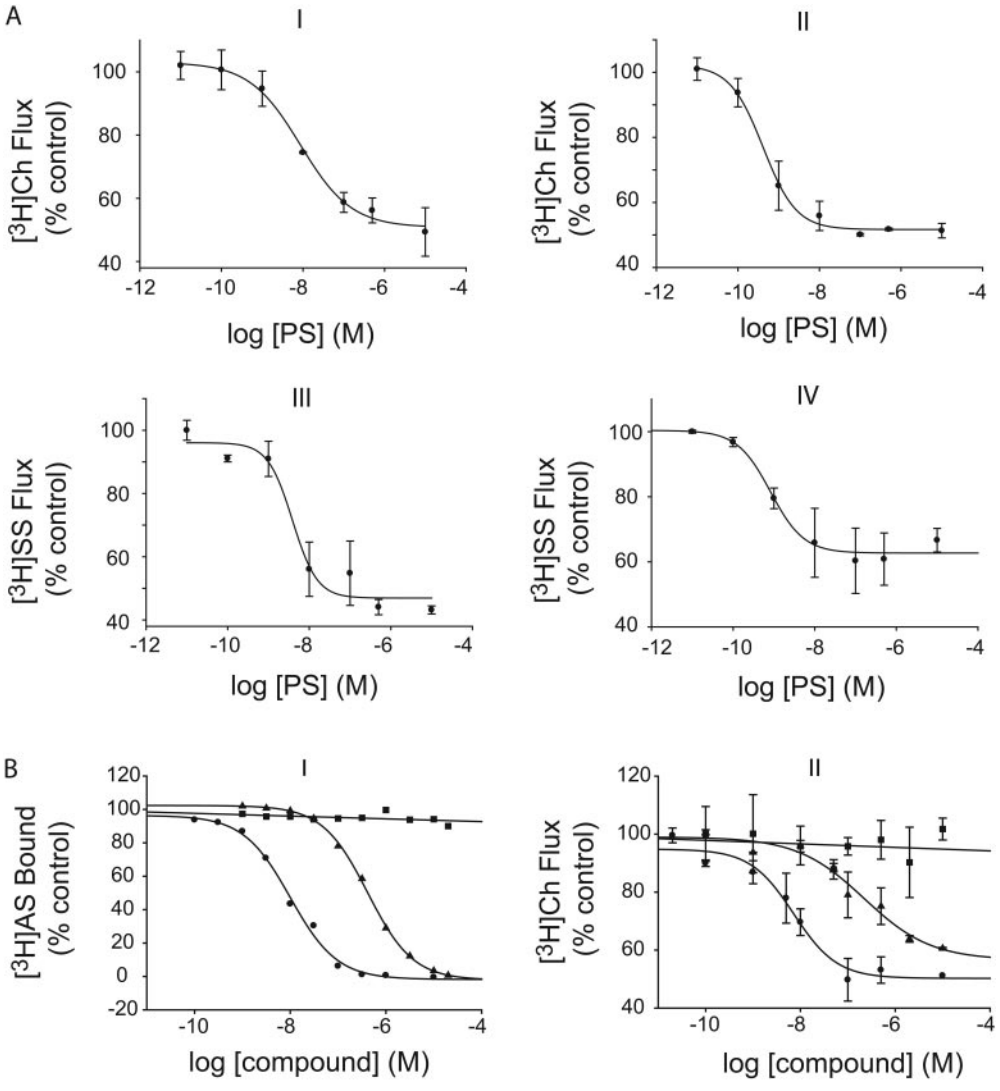

Fig. 7. Relationship between binding of EZE analogs to MDCKII cells overexpressing dog or human NPC1L1 and reduction of sterol flux. A, I and II, [^{3}H]cholesterol flux into human NPC1L1/MDCKII-Flp and dog NPC1L1/MDCKII-Flp cells. Cholesterol flux into human NPC1L1/MDCKII-Flp (I) and dog MDCKII-Flp (II) cells was performed as described in Fig. 6 in the presence of increasing concentrations of PS. [^{3}H]Ch flux was fit to a single-site inhibition model, yielding IC_{50} values of 10.3 nM (I) for hNPC1L1/MDCKII-Flp and 0.32 nM (II) for dNPC1L1/MDCKII-Flp, respectively. III and IV, [^{3}H]sitosterol flux into human NPC1L1/MDCKII-Flp and dog NPC1L1/MDCKII-Flp cells. [^{3}H]Sitosterol flux into human NPC1L1/MDCKII-Flp (III) and dog MDCKII-Flp (IV) cells was performed as described in Fig. 6, except for the replacement of [^{3}H]Ch with [^{3}H]sitosterol, in the presence of increasing concentrations of PS. [^{3}H]sitosterol flux was fit to a single-site inhibition model, yielding IC_{50} values of 5 nM (III) for hNPC1L1/MDCKII-Flp and 0.8 nM (IV) for dNPC1L1/MDCKII-Flp, respectively. B, correlation between binding affinity for human NPC1L1 and inhibition of cholesterol flux. Binding and flux experiments were performed as described above in (Figs. 6 and 7A). Specific [^{3}H]AS was fit to a single-site inhibition model, yielding K_i values of 5 nM (PS) (●), 209 nM (EZE-gluc) (▲) and N.D. (ent-1) (■). [^{3}H]Ch flux was fit to a single-site inhibition model, yielding IC_{50} values of values of 7 nM (PS) (●), 300 nM (EZE-gluc) (▲), and N.D. (ent-1) (■).

CKII cells as a robust source of endogenous NPC1L1-like activity with similar pharmacology to rat NPC1L1. Furthermore, and in agreement with a recent study, comparing the binding of glucuronidated ezetimibe to multiple species of NPC1L1 orthologs (Hawes et al., 2007), MDCKII cells, derived from dog distal convoluted tubule, were found to consistently bind EZE analogs more potently than rat NPC1L1 expressed in HEK293 cells. It is noteworthy that [^{3}H]AS binding to MDCKII cells occurs almost exclusively at the apical surface, consistent with the apparent localization of NPC1L1 in both enterocytes (Altmann et al., 2004) and hepatocytes (Yu et al., 2006).

Direct measurements using [^{3}H]AS indicate that serum-depleted MDCKII cells respond to inhibition of HMG CoA reductase by increasing the amount of NPC1L1 expressed at the cell surface. This observation supports and extends an analysis of the NPC1L1 promoter indicating that the HMG CoA reductase inhibitor mevinolin up-regulates transcription of NPC1L1 in CaCo-2 cells (Alrefai et al., 2007). It is noteworthy that this mechanism seems to be relevant only in cells grown in lipoprotein-depleted media, suggesting that under normal conditions, the acquisition of lipoproteins, cholesterol ester, and cholesterol through LDL receptor can bypass the need for up-regulating surface NPC1L1 levels. These observations support the contention that NPC1L1 may act as part of a cholesterol transport mechanism in MDCKII cells. However, unlike recent studies suggesting a rapid translocation of fluorescence-labeled human NPC1L1-GFP from inside the cell to the subapical membrane of McArdle RH7777 rat hepatoma cells (Yu et al., 2006; Brown et al., 2007), there was no short-term increase (<8 h) in the number of [^{3}H]AS binding sites in MDCKII II cells upon challenging with lovastatin (data not shown), which is consistent with a transcriptional response (Alrefai et al., 2007).

Although enterocytes and hepatocytes facilitate the transcellular flux of cholesterol (Huff et al., 2006; Davis and Veltri, 2007; Levy et al., 2007; Orlowski et al., 2007), MDCKII cells are derived from the kidney distal convoluted tubule where the apical membrane faces the filtration fluid, and cholesterol flux has not been reported. Given these differences in transcellular cholesterol flux, it was important to determine whether MDCKII cells, although sensing and responding to variations in endogenous cholesterol, could actually transport cholesterol in an NPC1L1-dependent manner. Using an assay similar to that reported for monitoring EZE-sensitive cholesterol influx into McArdle RH7777 rat hepatoma cells overexpressing human NPC1L1 tagged with GFP (Yu et al., 2006), cholesterol flux in the apical membrane of MDCKII cells, after cholesterol-depletion with βmCD, was not significantly sensitive to EZE (Yu et al., 2006). These observations indicate that at a defined NPC1L1 site density of 4×10^5 [^{3}H]AS sites/cell, there is not enough NPC1L1-dependent Ch influx into cells to overcome the endogenous incorporation of [^{3}H]Ch into the membrane of MDCKII cells. However, overexpression of dog or human NPC1L1 in MDCKII cells increases the amount of NPC1L1-mediated cholesterol influx relative to nonspecific delivery of cholesterol. Such an approach, in a manner similar to the overexpression of NPC1L1 in CaCo-2 cells (Yamanashi et al., 2007), allows the delivery of [^{3}H]cholesterol or [^{3}H]sitosterol to MDCKII cells in an EZE-sensitive manner and suggests that NPC1L1 is solely responsible for the increase in Ch influx in vitro.

By taking advantage of [^{3}H]AS to accurately define the affinity of EZE analog binding to NPC1L1 and EZE analogs to block [^{3}H]Ch flux through NPC1L1, we have been able to examine the pharmacological relationship between EZE analog binding to NPC1L1 and its effect on EZE analog sensitive cholesterol flux in vitro. It is remarkable that the IC_{50} of EZE analog block of cholesterol flux for both dog and mouse NPC1L1 is virtually identical to the K_d of EZE analog binding. This observation indicates a tight coupling between EZE analog binding and reduction in cholesterol flux, suggesting that mechanistically, EZE analogs reduce cholesterol flux through NPC1L1 by either competing directly with cholesterol to bind, presumably at the sterol-sensing domain (Radhakrishnan et al., 2004) or by altering critical conformational changes in NPC1L1 necessary for cholesterol flux. Discriminating between these hypotheses has critical implications for the design of novel NPC1L1 inhibitors.

Acknowledgments

We thank Herb Bull, Jane Chin, Bob Devita, Raymond Evers, Marga Garcia-Calvo, Jean-Marie Lisnock, Euan MacIntyre, Roger Meurer, Sandy Mills, Lyndon Mitnaul, Carl Sparrow, Nancy Thornberry, and Sam Wright for their important contributions to this research. We also thank Carl Sparrow and Sam Wright for their critical review of the manuscript. Finally, we thank Piet Borst for the kind gift of the MDCKII cells and Liqing Yu for advice on the functional assay.

References

Alrefai W, Annaba F, Sarwar Z, Dwivedi A, Saksena S, Singla A, Dudeja PK, and Gill R (2007) Modulation of human Niemann-Pick C1 like 1 gene expression by sterol: role of sterol regulatory element binding protein-2. *Am J Physiol Gastrointest Liver Physiol* **292:**G369–G376.

Altmann SW, Davis HR Jr, Zhu LJ, Yao X, Hoos LM, Tetzloff G, Iyer SP, Maguire M, Golovko A, Zeng M, et al. (2004) Niemann-Pick C1 like 1 protein is critical for intestinal cholesterol absorption. *Science* **303:**1201–1204.

Ballantyne CM, Houri J, Notarbartolo A, Melani L, Lipka LJ, Suresh R, Sun S, LeBeaut AP, Sager PT, and Veltri EP (2003) Effect of ezetimibe coadministered with atorvastatin in 628 patients with primary hypercholesterolemia: a prospective, randomized, double-blind trial. *Circulation* **107:**2409–2415.

Bays HE, Moore PB, Drehobl MA, Rosenblatt S, Toth PD, Dujovne CA, Knopp RH, Lipka LJ, Lebeaut AP, Yang B, et al. (2001) Effectiveness and tolerability of ezetimibe in patients with primary hypercholesterolemia: pooled analysis of two phase II studies. *Clin Ther* **23:**1209–1230.

Brown JM, Rudel LL, and Yu L (2007) NPC1L1 (Niemann-Pick C1-like 1) mediates sterol-specific unidirectional transport of non-esterified cholesterol in McArdle-RH7777 hepatoma cells. *Biochem J* **406:**273–283.

Chen CS, Bach G, and Pagano RE (1998) Abnormal transport along the lysosomal pathway in mucolipidosis, type IV disease. *Proc Natl Acad Sci U S A* **95:**6373–6378.

Chen WY, Bailey EC, McCune SL, Dong JY, and Townes TM (1997) Reactivation of silenced, virally transduced genes by inhibitors of histone deacetylase. *Proc Natl Acad Sci U S A* **94:**5798–5803.

Davidson MH, McGarry T, Bettis R, Melani L, Lipka LJ, LeBeaut AP, Suresh R, Sun S, and Veltri EP (2002) Ezetimibe coadministered with simvastatin in patients with primary hypercholesterolemia. *J Am Coll Cardiol* **40:**2125–2134.

Davies JP, Scott C, Oishi K, Liapis A, and Ioannou YA (2005) Inactivation of NPC1L1 causes multiple lipid transport defects and protects against diet-induced hypercholesterolemia. *J Biol Chem* **280:**12710–12720.

Davis HR and Veltri EP (2007) Zetia: inhibition of Niemann-Pick C1 Like 1 (NPC1L1) to reduce intestinal cholesterol absorption and treat hyperlipidemia. *J Atheroscler Thromb* **14:**99–108.

Dujovne CA, Ettinger MP, McNeer JF, Lipka LJ, LeBeaut AP, Suresh R, Yang B, and Veltri EP (2002) Efficacy and safety of a potent new selective cholesterol absorption inhibitor, ezetimibe, in patients with primary hypercholesterolemia. *Am J Cardiol* **90:**1092–1097.

During A, Dawson HD, and Harrison EH (2005) Carotenoid transport is decreased and expression of the lipid transporters SR-BI, NPC1L1, and ABCA1 is downregulated in Caco-2 cells treated with ezetimibe. *J Nutr* **135:**2305–2312.

Duval C, Touche V, Tailleux A, Fruchart JC, Fievet C, Clavey V, Staels B, and Lestavel S (2006) Niemann-Pick C1 like 1 gene expression is down-regulated by LXR activators in the intestine. *Biochem Biophys Res Commun* **340:**1259–1263.

Field FJ, Watt K, and Mathur SN (2007) Ezetimibe interferes with cholesterol trafficking from the plasma membrane to the endoplasmic reticulum in CaCo-2 cells. *J Lipid Res* **48:**1735–1745.

Gagné C, Bays HE, Weiss SR, Mata P, Quinto K, Melino M, Cho M, Musliner TA, and Gumbiner B (2002) Efficacy and safety of ezetimibe added to ongoing statin

therapy for treatment of patients with primary hypercholesterolemia. *Am J Cardiol* **90:**1084–1091.
Garcia-Calvo M, Lisnock J, Bull HG, Hawes BE, Burnett DA, Braun MP, Crona JH, Davis HR Jr, Dean DC, Detmers PA, et al. (2005) The target of ezetimibe is Niemann-Pick C1-Like 1 (NPC1L1). *Proc Natl Acad Sci U S A* **102:**8132–8137.
Garmy N, Taieb N, Yahi N, and Fantini J (2005) Interaction of cholesterol with sphingosine: physicochemical characterization and impact on intestinal absorption. *J Lipid Res* **46:**36–45.
Goulet MT, Ujjainwalla F, von Langen D, and Ogawa A (2005), inventors; Merck & Co, Goulet MT, Ujjainwalla F, von Langen D, and Ogawa A, assignees. Anti-hypercholesterolemic compounds. World Patent number WO2005062824. 2005 July 14.
Grundy SM (1983) Absorption and metabolism of dietary cholesterol. *Annu Rev Nutr* **3:**71–96.
Hanner M, Green B, Gao YD, Schmalhofer WA, Matyskiela M, Durand DJ, Felix JP, Linde AR, Bordallo C, Kaczorowski GJ, et al. (2001) Binding of correolide to the K(v)1.3 potassium channel: characterization of the binding domain by site-directed mutagenesis. *Biochemistry* **40:**11687–11697.
Hawes BE, O'Neill KA, Yao X, Crona JH, Davis HR Jr, Graziano MP, and Altmann SW (2007) In vivo responsiveness to ezetimibe correlates with Niemann-Pick C1 Like-1 (NPC1L1) binding affinity: comparison of multiple species NPC1L1 orthologs. *Mol Pharmacol* **71:**19–29.
Hopkins CR and Trowbridge IS (1983) Internalization and processing of transferrin and the transferrin receptor in human carcinoma A431 cells. *J Cell Biol* **97:**508–521.
Huff MW, Pollex RL, and Hegele RA (2006) NPC1L1: evolution from pharmacological target to physiological sterol transporter. *Arterioscler Thromb Vasc Biol* **26:**2433–2438.
Iyer SP, Yao X, Crona JH, Hoos LM, Tetzloff G, Davis HR Jr., Graziano MP, and Altmann SW (2005) Characterization of the putative native and recombinant rat sterol transporter Niemann-Pick C1 Like 1 (NPC1L1) protein. *Biochim Biophys Acta* **1722:**282–292.
Kerzner B, Corbelli J, Sharp S, Lipka LJ, Melani L, LeBeaut A, Suresh R, Mukhopadhyay P, and Veltri EP (2003) Efficacy and safety of ezetimibe coadministered with lovastatin in primary hypercholesterolemia. *Am J Cardiol* **91:**418–424.
Knaus HG, Koch RO, Eberhart A, Kaczorowski GJ, Garcia ML, and Slaughter RS (1995) [^{125}I]Margatoxin, an extraordinarily high affinity ligand for voltage-gated potassium channels in mammalian brain. *Biochemistry* **34:**13627–13634.
Knöpfel M, Davies JP, Duong PT, Kvaerno L, Carreira EM, Phillips MC, Ioannou YA, and Hauser H (2007) Multiple plasma membrane receptors but not NPC1L1 mediate high-affinity, ezetimibe-sensitive cholesterol uptake into the intestinal brush border membrane. *Biochim Biophys Acta* **1771:**1140–1147.
Knopp RH, Gitter H, Truitt T, Bays H, Manion CV, Lipka LJ, LeBeaut AP, Suresh R, Yang B, and Veltri EP (2003) Effects of ezetimibe, a new cholesterol absorption inhibitor, on plasma lipids in patients with primary hypercholesterolemia. *Eur Heart J* **24:**729–741.
Labonté ED, Howles PN, Granholm NA, Rojas JC, Davies JP, Ioannou YA, and Hui DY (2007) Class B type I scavenger receptor is responsible for the high affinity cholesterol binding activity of intestinal brush border membrane vesicles. *Biochim Biophys Acta* **1771:**1132–1139.
Levy E, Spahis S, Sinnett D, Peretti N, Maupas-Schwalm F, Delvin E, Lambert M, and Lavoie MA (2007) Intestinal cholesterol transport proteins: an update and beyond. *Curr Opin Lipidol* **18:**310–318.
Louvard D (1980) Apical membrane aminopeptidase appears at site of cell-cell contact in cultured kidney epithelial cells. *Proc Natl Acad Sci U S A* **77:**4132–4136.
Mathur SN, Watt KR, and Field FJ (2007) Regulation of intestinal NPC1L1 expression by dietary fish oil and docosahexaenoic acid. *J Lipid Res* **48:**395–404.
Melani L, Mills R, Hassman D, Lipetz R, Lipka L, LeBeaut A, Suresh R, Mukhopadhyay P, and Veltri E (2003) Efficacy and safety of ezetimibe coadministered with pravastatin in patients with primary hypercholesterolemia: a prospective, randomized, double-blind trial. *Eur Heart J* **24:**717–728.
Orlowski S, Comera C, Terce F, and Collet X (2007) Lipid rafts: dream or reality for cholesterol transporters? *Eur Biophys J* **36:**869–885.
Priest BT, Garcia ML, Middleton RE, Brochu RM, Clark S, Dai G, Dick IE, Felix JP, Liu CJ, Reiseter BS, et al. (2004) A disubstituted succinamide is a potent sodium channel blocker with efficacy in a rat pain model. *Biochemistry* **43:**9866–9876.
Radhakrishnan A, Sun LP, Kwon HJ, Brown MS, and Goldstein JL (2004) Direct binding of cholesterol to the purified membrane region of SCAP: mechanism for a sterol-sensing domain. *Mol Cell* **15:**259–268.
Sané AT, Sinnett D, Delvin E, Bendayan M, Marcil V, Menard D, Beaulieu JF, and Levy E (2006) Localization and role of NPC1L1 in cholesterol absorption in human intestine. *J Lipid Res* **47:**2112–2120.
Simon-Assmann P, Turck N, Sidhoum-Jenny M, Gradwohl G, and Kedinger M (2007) In vitro models of intestinal epithelial cell differentiation. *Cell Biol Toxicol* **23:**241–256.
Smith MM and Levitan DJ (2007) Human NPC1L1 and NPC1 can functionally substitute for the ncr genes to promote reproductive development in C. elegans. *Biochim Biophys Acta* **1770:**1345–1351.
van der Veen JN, Kruit JK, Havinga R, Baller JF, Chimini G, Lestavel S, Staels B, Groot PH, Groen AK, and Kuipers F (2005) Reduced cholesterol absorption upon PPARdelta activation coincides with decreased intestinal expression of NPC1L1. *J Lipid Res* **46:**526–534.
Yamanashi Y, Takada T, and Suzuki H (2007) NPC1L1 over-expression facilitates ezetimibe-sensitive cholesterol and {beta}-sitosterol uptake in CaCo-2 cells. *J Pharmacol Exp Ther* **320:**559–564.
Yu L, Bharadwaj S, Brown JM, Ma Y, Du W, Davis MA, Michaely P, Liu P, Willingham MC, and Rudel LL (2006) Cholesterol-regulated translocation of NPC1L1 to the cell surface facilitates free cholesterol uptake. *J Biol Chem* **281:**6616–6624.

Address correspondence to: Adam B. Weinglass, Department of Ion Channels, Merck Research Laboratories, P.O. Box 2000, Rahway, NJ 07065. E-mail: adam_weinglass@merck.com